Refined theories based on non-polynomial kinematics for the thermoelastic analysis of functionally graded plates

(Article begins on next page)

20 April 2024

Refined theories based on non-polynomial kinematics for the thermoelastic analysis of functionally graded plates

I.A. Ramos [1], J.L. Mantari [2], A. Pagani[3] and E. Carrera[3*]

[1]*Faculty of Mechanical Engineering, Universidad Nacional de Ingeniería, Av. Túpac Amaru 210, Rimac, Peru*

[2]*Faculty of Mechanical Engineering, Universidad de Ingeniería y Tecnología (UTEC), Santa Anita, Lima, Peru*

[3]*Department of Mechanical and Aerospace Engineering, Politecnico di Torino, Torino, Italy*

Abstract

This paper presents an analytical solution for the thermoelastic analysis of simply-supported functionally graded sandwich plates using the Carrera Unified Formulation (CUF), which allows the automatic implementation of various structural theories. The governing equations for plates under thermal loads are obtained by using the principal of virtual displacement and solved using the Navier method. Linear and non-linear temperature fields through the thickness are taken into account. Particular attention is focused on plate theories with non-polynomial refined kinematics. The results of the present displacement fields are compared with the classical polynomial ones, proposed by Carrera, for several orders of expansion.

.

*Address correspondence to Prof. Erasmo Carrera, Department of Mechanical and Aerospace Engineering, Politecnico di Torino, Corso Duca degli Abruzzi 24, 10129 Torino, Italy. E-mail: erasmo.carrera@polito.it

INTRODUCTION

Functionally graded materials (FGMs) are a kind of advanced composite materials formed of two or more constituent phases with a continuously variable distribution by gradually changing the volume fraction. The conventional laminated materials suffer from discontinuity of materials properties between the layers. As a result, stress concentration occurs at the interface. FGMs were born to eliminate the problems due to bonding of two discrete materials [1].

There are various theories and different variational statements to study the mechanical behavior of FGMs [2, 3]. For example, the classical plate theory or Kirchoff theory, which ignores the normal and shear deformation effect, only give acceptable results for thin plates. Then, the first order shear deformation theory (FSDT) devised by Raissner and Mindlin has been widely adopted in the literature, but this theory needs a shear correction factor which is difficult to calculate. Therefore, higher-order shear deformation theories (HSDTs) were introduced to accurately describe the shear deformation effects. The HSDTs can be classified in different classes, such as equivalent single layer (ESL), quasi-layer-wise and layer-wise models [4-8]. Further, the HSDTs can be developed using polynomial [9, 10] or non-polynomial kinematics [11-20].

The thermoelastic problem of FG sandwich plates were studied by Zenkour and Alghamdi [21], Houari et al. [22] and Mantari and Granados [23] using a HSDT with thickness stretching effect and a non-linear thermal distribution.

CUF was formulated by Carrera for laminated plates and shells [24-26] which offers a procedure to implement several plate and shell theories by expanding the displacement variables in the thickness coordinate using generic functions, originally Taylor's expansions of N-order. The CUF was further implemented to study FGM in

[27] and both PVD and Raissner's mixed variational statements have been utilized in Carrera's works. A sinusoidal shear deformation theory (SSDT) within the CUF framework was developed by Ferreira et al. [28] for static and free vibration analysis of laminated shells. The SSDT accounts for through-the-thickness deformation, by considering sinusoidal variation of all displacements. Neves et al. [29, 30] used a similar theory of Ferreira to study the bending and free vibration of functionally graded plates (FGPs). Their formulations are based on hybrid quasi-3D sinusoidal shear deformation theory with a quadratic variation across the thickness. A quasi-3D hyperbolic shear deformation theory for the static and free vibration analysis of FGPs, similar to the previous theory [29, 30], was developed by Neves et al. [31, 32]. Static analysis for several theories based on trigonometric, hyperbolic, exponential and zig-zag function were developed by Carrera et al. [33] for laminated beams and Filippi et al. [34] for FGM beams. Furthermore, Mashat et al. [35] presented free vibration analysis of FGM beams by various theories.

A thermal stability analysis of FG sandwich plates was developed by Fazzolari and Carrera [36] using CUF and several nonlinear thermal distribution forms.

By employing CUF, this paper proposes several plate theories and analytical solutions for thermoelastic analysis of simply supported FG sandwich plates. This work proposes sinusoidal and hyperbolic functions in normalized ($sin^n(z/h)$, $sin(nz/h)$, $sinh^n(z/h)$ and $sinh(nz/h)$) and non-normalized ($sin^n(z)$, $sin(nz)$, $sinh^n(z)$ and $sinh(nz)$) forms. Further, hybrid functions ($sec(z/h)$, $tanh(z/h)$, $sec(z)$ and $tanh(z)$) are proposed and compared with the polynomial kinematics for several order of expansions (N=3, 4, 5, 6, 7). Linear and non-linear temperature field through the thickness are taken into account. The mechanical properties of the FGPs vary a cross the thickness direction according to a power law distribution in terms of volume fraction. The governing

equations for the static analysis are obtained through PVD, and solved using the Navier solution method.

The paper is organized as follows. Section 2 outlines the mathematical modeling under CUF framework. Theoretical formulation of FGMs, displacement field, kinematic, constitutive relations, the principle of virtual works, and the governing equations are presented. Section 3 describes the analytical solution methodology. Section 4 is about results and discussions. Finally, further general aspects are given in the conclusions.

ANALYTICAL MODELLING

In a FGP, the mechanical properties can be smoothly graded from different directions and considering different shapes. This paper considers the well-known across the thickness gradation modeling of the mechanical properties of FGPs, resulting in sandwich plates made of an isotropic material (fully metal) in the core and a FGM in the bottom and top skins. The rectangular sandwich plate has uniform thickness "h", length "a", and width "b", and it is shown in Fig. 1. The rectangular Cartesian coordinate system x, y, z, has the plane xy at z = 0, coinciding with the mid-surface of the plate.

Functionally graded plates (FGPs)

The material properties can vary through the thickness with a power law distribution, which is defined as follows:

$$P_{(z)} = (P_t - P_b)V_{c(z)} + P_b$$

$$V_{c(z)} = \begin{cases} \left(\dfrac{z - h_1}{h_2 - h_1}\right)^p & h_1 \leq z \leq h_2 \\ 1 & h_2 \leq z \leq h_3 \\ \left(\dfrac{z - h_4}{h_3 - h_4}\right)^p & h_3 \leq z \leq h_4 \end{cases} \tag{1}$$

where $P(z)$ denotes the effective material property across the thickness, P_t and P_b denote the correspondent property at the top and bottom faces of the plate, and p is the exponent that specifies the material variation profile through the thickness. The effective material properties of the plate that vary according to Eq. (1) are the Young's modulus E, the shear modulus G, and the thermal expansion coefficients α. In Eq. (1), $V_c(z)$ is the volume fraction of the ceramic material, see Fig. 2. The Poisson ratio, ν is assumed to be constant.

Refined kinematics models

CUF states that the displacement field for plates, $\boldsymbol{u}(x, y, z)$, can modeled as a generic expansion of generic through-the-thickness functions, $f_\tau(z)$.

$$\boldsymbol{u}(x, y, z) = f_s(z)\, \boldsymbol{u}_s(x, y), \quad s = 0, 1, \ldots, M$$

$$\delta\boldsymbol{u}(x, y, z) = f_\tau(z)\delta\boldsymbol{u}_\tau(x, y), \quad \tau = 0, 1, \ldots, M \tag{2}$$

$\boldsymbol{u}_s$ is the displacement vector and $\delta\boldsymbol{u}_\tau$ the relative variation. M stands for the number of expansion terms. According to Einstein's notation, the repeated subscript τ and s indicate summation. For example, in the case of $M = 7$, the displacement field is

$$u_x = f_{0(z)}u_{x_0} + f_{1(z)}u_{x_1} + f_{2(z)}u_{x_2} + \cdots + f_{7(z)}u_{x_7}$$

5

$$u_y = f_{0(z)}u_{y_0} + f_{1(z)}u_{y_1} + f_{2(z)}u_{y_2} + \cdots + f_{7(z)}u_{y_7}$$

$$u_z = f_{0(z)}u_{z_0} + f_{1(z)}u_{z_1} + f_{2(z)}u_{z_2} + \cdots + f_{7(z)}u_{z_7} \tag{3}$$

In several works about CUF (see for example Carrera et. al. [37]) polynomial functions have been adopted to develop refined plate theories (i.e., $f_n = z^n$). This class of polynomials expansion models have demonstrated their validity and accuracy in several works. In this paper, non-polynomial functions are employed as $f_\tau(z)$, see Table 1.

Elastic displacement-strain relation and constitutive law

The stress (σ^k) and the strain (ε^k) of the k$^{\text{th}}$ layer are grouped as follows:

$$\boldsymbol{\sigma}_p^k = \begin{bmatrix} \sigma_{xx}^k & \sigma_{yy}^k & \sigma_{xy}^k \end{bmatrix}^T$$

$$\boldsymbol{\sigma}_n^k = \begin{bmatrix} \sigma_{xz}^k & \sigma_{yz}^k & \sigma_{zz}^k \end{bmatrix}^T \tag{4}$$

$$\boldsymbol{\varepsilon}_p^k = \begin{bmatrix} \varepsilon_{xx}^k & \varepsilon_{yy}^k & \varepsilon_{xy}^k \end{bmatrix}^T$$

$$\boldsymbol{\varepsilon}_n^k = \begin{bmatrix} \varepsilon_{xz}^k & \varepsilon_{yz}^k & \varepsilon_{zz}^k \end{bmatrix}^T$$

Subscript "n" is related to the in-plane components, while "p" to the out-of-plane components. The strain-displacement relationship are given as:

$$\boldsymbol{\varepsilon}_p^k = \boldsymbol{D}_p \boldsymbol{u}^k$$

$$\boldsymbol{\varepsilon}_n^k = \boldsymbol{D}_n \boldsymbol{u}^k = (\boldsymbol{D}_{np} + \boldsymbol{D}_{nz})\boldsymbol{u}^k \tag{5}$$

$$
\boldsymbol{D}_p = \begin{bmatrix} \dfrac{\partial}{\partial x} & 0 & 0 \\[2mm] 0 & \dfrac{\partial}{\partial y} & 0 \\[2mm] \dfrac{\partial}{\partial y} & \dfrac{\partial}{\partial x} & 0 \end{bmatrix}, \qquad
\boldsymbol{D}_{np} = \begin{bmatrix} 0 & 0 & \dfrac{\partial}{\partial x} \\[2mm] 0 & 0 & \dfrac{\partial}{\partial y} \\[2mm] 0 & 0 & 0 \end{bmatrix}, \qquad
\boldsymbol{D}_{nz} = \begin{bmatrix} \dfrac{\partial}{\partial z} & 0 & 0 \\[2mm] 0 & \dfrac{\partial}{\partial z} & 0 \\[2mm] 0 & 0 & \dfrac{\partial}{\partial z} \end{bmatrix}
$$

For FGPs, the stress-strain relationship of the k$^{\text{th}}$ layer can be expressed as:

$$
\begin{bmatrix} \sigma_{xx}^k \\ \sigma_{yy}^k \\ \sigma_{xy}^k \\ \sigma_{xz}^k \\ \sigma_{yz}^k \\ \sigma_{zz}^k \end{bmatrix} =
\begin{bmatrix}
C_{11}^k(z) & C_{12}^k(z) & 0 & 0 & 0 & C_{13}^k(z) \\
C_{12}^k(z) & C_{22}^k(z) & 0 & 0 & 0 & C_{23}^k(z) \\
0 & 0 & C_{66}^k(z) & 0 & 0 & C_{36}^k(z) \\
0 & 0 & 0 & C_{55}^k(z) & 0 & 0 \\
0 & 0 & 0 & 0 & C_{44}^k(z) & 0 \\
C_{13}^k(z) & C_{23}^k(z) & C_{36}^k(z) & 0 & 0 & C_{33}^k(z)
\end{bmatrix}
\begin{bmatrix} \varepsilon_{xx}^k - \alpha^k T^k \\ \varepsilon_{yy}^k - \alpha^k T^k \\ \varepsilon_{xy}^k \\ \varepsilon_{xz}^k \\ \varepsilon_{yz}^k \\ \varepsilon_{zz}^k - \alpha^k T^k \end{bmatrix}
\tag{6}
$$

where T^k is the temperature field within the layer. The temperature varies through the thickness of the plate with the following temperature:

$$
T(x,y,z) = T_1(x,y) + \frac{z}{h} T_2(x,y) + \frac{\psi(z)}{h} T_3(x,y)
$$

$$
T(x,y,z) = F_\theta(z) T_\theta(x,y) \qquad \theta = 1,2,3
\tag{7}
$$

where $F_1 = 1$, $F_2 = z/h$, $F_3 = \psi/h$. T_1, T_2 and T_3 are thermal loads. The expressions of $C_{ij}^k(z)$ are given below:

$$
C_{11}^k(z) = C_{22}^k(z) = C_{33}^k(z) = \frac{E(z)(1-v)}{(1-2v)(1+v)}
$$

$$C_{13}^k(z) = C_{23}^k(z) = C_{36}^k(z) = \frac{E(z)\,\nu}{(1-2\nu)(1+\nu)} \tag{8}$$

$$C_{55}^k(z) = C_{44}^k(z) = C_{66}^k(z) = \frac{E(z)}{2(1+\nu)}$$

According to Eq. (4), Eq. (6) becomes:

$$\boldsymbol{\sigma}_p^k = \left(\boldsymbol{C}_{pp}^k \boldsymbol{\varepsilon}_p^k + \boldsymbol{C}_{pn}^k \boldsymbol{\varepsilon}_n^k\right) - \left(\boldsymbol{C}_{pp}^k \boldsymbol{\alpha}_p^k + \boldsymbol{C}_{pn}^k \boldsymbol{\alpha}_n^k\right) T^k$$

$$\boldsymbol{\sigma}_n^k = \left(\boldsymbol{C}_{np}^k \boldsymbol{\varepsilon}_p^k + \boldsymbol{C}_{nn}^k \boldsymbol{\varepsilon}_n^k\right) - \left(\boldsymbol{C}_{np}^k \boldsymbol{\alpha}_p^k + \boldsymbol{C}_{nn}^k \boldsymbol{\alpha}_n^k\right) T^k \tag{9}$$

where:

$$\boldsymbol{C}_{pp}^k = \begin{bmatrix} C_{11(z)}^k & C_{12(z)}^k & 0 \\ C_{12(z)}^k & C_{22(z)}^k & 0 \\ 0 & 0 & C_{66(z)}^k \end{bmatrix}^k \qquad \boldsymbol{C}_{nn}^k = \begin{bmatrix} C_{55(z)}^k & 0 & 0 \\ 0 & C_{44(z)}^k & 0 \\ 0 & 0 & C_{33(z)}^k \end{bmatrix}^k$$

$$\boldsymbol{C}_{np}^k = \begin{bmatrix} 0 & 0 & 0 \\ 0 & 0 & 0 \\ C_{13(z)}^k & C_{23(z)}^k & C_{36(z)}^k \end{bmatrix}^k \qquad \boldsymbol{C}_{pn}^k = \begin{bmatrix} 0 & 0 & C_{13(z)}^k \\ 0 & 0 & C_{23(z)}^k \\ 0 & 0 & C_{36(z)}^k \end{bmatrix}^k$$

$$\boldsymbol{\alpha}_n^k = \begin{bmatrix} 0 \\ 0 \\ \alpha^k \end{bmatrix} \qquad \boldsymbol{\alpha}_p^k = \begin{bmatrix} \alpha^k \\ \alpha^k \\ 0 \end{bmatrix} \tag{10}$$

Principle of virtual works

In the case of static analysis, the PVD yields

$$\sum_{k=1}^{N_l} \int_{\Omega_k} \int_{A_k} \left\{ \delta\boldsymbol{\varepsilon}_p^{k^T} \boldsymbol{\sigma}_p^k + \delta\boldsymbol{\varepsilon}_n^{k^T} \boldsymbol{\sigma}_n^k \right\} d\Omega_k dz = \sum_{k=1}^{N_l} \delta L_e^k \tag{11}$$

8

Where Ω_k is the layer mean are in the xy-plane, A_k denotes the k-layer thickness domain, N_l stands for the number of layers, and δL_e^k is the virtual variation of the external work. This paper only considers thermal effects, so $\delta L_e^k = 0$.

By using Eqs. (9) and (5), for a generic layer k, Eq. (11) becomes:

$$\int_{\Omega_k} \int_{A_k} \left\{ (D_p \delta u^k)^T \left[\left(C_{pp}^k D_p + C_{pn}^k (D_{np} + D_{nz}) \right) u^k - (C_{pp}^k \alpha_p^k + C_{pn}^k \alpha_n^k) T^k \right] \right.$$

$$+ \left((D_{np} + D_{nz}) \delta u^k \right)^T \left[\left(C_{np}^k D_p + C_{nn}^k (D_{np} + D_{nz}) \right) u^k \right. \tag{12}$$

$$\left. \left. - (C_{np}^k \alpha_p^k + C_{nn}^k \alpha_n^k) T^k \right] \right\} d\Omega_k dz = 0$$

By substituting Eqs. (2) and (7) into Eq. (12) and introducing the following notation:

$$\left(E_{\tau s pp}^k, E_{\tau s pn}^k, E_{\tau s_{,z} pn}^k \right) = \int_{A_k} (F_\tau F_s C_{pp}^k, F_\tau F_s C_{pn}^k, F_\tau F_{s_{,z}} C_{pn}^k) dz$$

$$\left(E_{\tau s np}^k, E_{\tau s nn}^k, E_{\tau s_{,z} nn}^k \right) = \int_{A_k} (F_\tau F_s C_{np}^k, F_\tau F_s C_{nn}^k, F_\tau F_{s_{,z}} C_{nn}^k) dz$$

$$\left(E_{\tau_{,z} s np}^k, E_{\tau_{,z} s nn}^k, E_{\tau_{,z} s_{,z} nn}^k \right) = \int_{A_k} (F_{\tau_{,z}} F_s C_{np}^k, F_{\tau_{,z}} F_s C_{nn}^k, F_{\tau_{,z}} F_{s_{,z}} C_{nn}^k) dz$$

$$\left(R_{\tau \theta pp}^k, R_{\tau \theta pn}^k \right) = \int_{A_k} \left(F_\tau F_\theta C_{pp}^k \alpha_p^k, F_\tau F_\theta C_{pn}^k \alpha_n^k \right) dz$$

$$\left(R_{\tau \theta np}^k, R_{\tau \theta nn}^k \right) = \int_{A_k} \left(F_\tau F_\theta C_{np}^k \alpha_p^k, F_\tau F_\theta C_{nn}^k \alpha_n^k \right) dz$$

$$\left(R_{\tau_{,z} \theta np}^k, R_{\tau_{,z} \theta nn}^k \right) = \int_{A_k} \left(F_{\tau_{,z}} F_\theta C_{np}^k \alpha_p^k, F_{\tau_{,z}} F_\theta C_{nn}^k \alpha_n^k \right) dz \tag{13}$$

one has

$$\int_{\Omega_k} \left\{ \left(\boldsymbol{D_p}\delta\boldsymbol{u_\tau^k}\right)^T \left(\boldsymbol{E_{\tau spp}^k}\boldsymbol{D_p}\boldsymbol{u_s^k} + \boldsymbol{E_{\tau spn}^k}\boldsymbol{D_{np}}\boldsymbol{u_s^k} + \boldsymbol{E_{\tau s,zpn}^k}\boldsymbol{u_s^k}\right) \right.$$

$$+ \left(\boldsymbol{D_{np}}\delta\boldsymbol{u_\tau^k}\right)^T \left(\boldsymbol{E_{\tau snp}^k}\boldsymbol{D_p}\boldsymbol{u_s^k} + \boldsymbol{E_{\tau snn}^k}\boldsymbol{D_{np}}\boldsymbol{u_s^k} + \boldsymbol{E_{\tau s,znn}^k}\boldsymbol{u_s^k}\right)$$

$$+ \left(\delta\boldsymbol{u_\tau^k}\right)^T \left(\boldsymbol{E_{\tau,zsnp}^k}\boldsymbol{D_p}\boldsymbol{u_s^k} + \boldsymbol{E_{\tau,zsnn}^k}\boldsymbol{D_{np}}\boldsymbol{u_s^k} + \boldsymbol{E_{\tau,zs,znn}^k}\boldsymbol{u_s^k}\right) \right\} d\Omega_k \tag{14}$$

$$- \int_{\Omega_k} \left\{ \left(\boldsymbol{D_p}\delta\boldsymbol{u_\tau^k}\right)^T \left(\boldsymbol{R_{\tau\theta pp}^k}\boldsymbol{T_\theta^k} + \boldsymbol{R_{\tau\theta pn}^k}\boldsymbol{T_\theta^k}\right) + \left(\boldsymbol{D_{np}}\delta\boldsymbol{u_\tau^k}\right)^T \left(\boldsymbol{R_{\tau,z\theta np}^k}\boldsymbol{T_\theta^k} \right. \right.$$

$$\left. + \boldsymbol{R_{\tau,z\theta nn}^k}\boldsymbol{T_\theta^k}\right) + \left(\delta\boldsymbol{u_\tau^k}\right)^T \left(\boldsymbol{R_{\tau,z\theta np}^k}\boldsymbol{T_\theta^k} + \boldsymbol{R_{\tau,z\theta nn}^k}\boldsymbol{T_\theta^k}\right) \right\} d\Omega_k = 0$$

where z after the comma indicates partial derivative. Integrating by parts and denoting the layer edges domain with $\varGamma_k$, Eq. (14) becomes:

$$\int\limits_{\Omega_k} \left\{ (\delta\boldsymbol{u}_\tau^k)^T \left(-(\boldsymbol{D}_p)^T \left[\boldsymbol{E}_{\tau spp}^k \boldsymbol{D}_p + \boldsymbol{E}_{\tau spn}^k \boldsymbol{D}_{np} + \boldsymbol{E}_{\tau S,z pn}^k \right] \right.\right.$$

$$- (\boldsymbol{D}_{np})^T \left[\boldsymbol{E}_{\tau snp}^k \boldsymbol{D}_p + \boldsymbol{E}_{\tau snn}^k \boldsymbol{D}_{np} + \boldsymbol{E}_{\tau S,z nn}^k \right]$$

$$\left.+ \left[\boldsymbol{E}_{\tau,z snp}^k \boldsymbol{D}_p + \boldsymbol{E}_{\tau,z snn}^k \boldsymbol{D}_{np} + \boldsymbol{E}_{\tau,z S,z nn}^k \right] \right) \boldsymbol{u}_s^k \right\} d\Omega_k$$

$$+ \int\limits_{\Gamma_k} \left\{ (\delta\boldsymbol{u}_\tau^k)^T \left((\boldsymbol{I}_p)^T \left[\boldsymbol{E}_{\tau spp}^k \boldsymbol{D}_p + \boldsymbol{E}_{\tau spn}^k \boldsymbol{D}_{np} + \boldsymbol{E}_{\tau S,z pn}^k \right] \right.\right.$$

$$\left.\left.+ (\boldsymbol{I}_{np})^T \left[\boldsymbol{E}_{\tau snp}^k \boldsymbol{D}_p + \boldsymbol{E}_{\tau snn}^k \boldsymbol{D}_{np} + \boldsymbol{E}_{\tau S,z nn}^k \right] \right) \boldsymbol{u}_s^k \right\} d\Gamma_k$$

$$- \int\limits_{\Omega_k} \left\{ (\delta\boldsymbol{u}_\tau^k)^T \left(-(\boldsymbol{D}_p)^T (\boldsymbol{R}_{\tau\theta pp}^k + \boldsymbol{R}_{\tau\theta pn}^k) \right.\right.$$

$$- (\boldsymbol{D}_{np})^T \left(\boldsymbol{R}_{\tau,z \theta np}^k + \boldsymbol{R}_{\tau,z \theta nn}^k \right)$$

$$\left.\left.+ \left(\boldsymbol{R}_{\tau,z \theta np}^k + \boldsymbol{R}_{\tau,z \theta nn}^k \right) \right) T_\theta^k \right\} d\Omega_k$$

$$- \int\limits_{\Gamma_k} \left\{ (\delta\boldsymbol{u}_\tau^k)^T \left((\boldsymbol{I}_p)^T (\boldsymbol{R}_{\tau\theta pp}^k + \boldsymbol{R}_{\tau\theta pn}^k) \right.\right.$$

$$\left.\left.+ (\boldsymbol{I}_{np})^T \left(\boldsymbol{R}_{\tau,z \theta np}^k + \boldsymbol{R}_{\tau,z \theta nn}^k \right) \right) T_\theta^k \right\} d\Gamma_k = 0$$

(15)

Accordingly, the governing equations and the related boundary conditions are written in the following form:

$$\int\limits_{\Omega_k} \left\{ (\delta\boldsymbol{u}_\tau^k)^T \boldsymbol{K}_{uu}^{k\tau s} \boldsymbol{u}_s^k \right\} d\Omega_k + \int\limits_{\Gamma_k} \left\{ (\delta\boldsymbol{u}_\tau^k)^T \boldsymbol{\Pi}_{uu}^{k\tau s} \boldsymbol{u}_s^k \right\} d\Gamma_k - \int\limits_{\Omega_k} \left\{ (\delta\boldsymbol{u}_\tau^k)^T \boldsymbol{K}_{u\theta}^{k\tau} T_\theta^k \right\} d\Omega_k$$

$$- \int\limits_{\Gamma_k} \left\{ (\delta\boldsymbol{u}_\tau^k)^T \boldsymbol{\Pi}_{u\theta}^{k\tau} T_\theta^k \right\} d\Gamma_k = 0$$

(16)

where:

11

$$K_{uu}^{k\tau s} = -(D_p)^T [E_{\tau spp}^k D_p + E_{\tau spn}^k D_{np} + E_{\tau S,z pn}^k]$$

$$- (D_{np})^T [E_{\tau snp}^k D_p + E_{\tau snn}^k D_{np} + E_{\tau S,z nn}^k] \tag{17a}$$

$$+ [E_{\tau,z snp}^k D_p + E_{\tau,z snn}^k D_{np} + E_{\tau,z S,z nn}^k]$$

$$\Pi_{uu}^{k\tau s} = (I_p)^T [E_{\tau spp}^k D_p + E_{\tau spn}^k D_{np} + E_{\tau S,z pn}^k]$$

$$+ (I_{np})^T [E_{\tau snp}^k D_p + E_{\tau snn}^k D_{np} + E_{\tau S,z nn}^k] \tag{17b}$$

$$K_{u\theta}^{k\tau\theta} = -(D_p)^T (R_{\tau\theta pp}^k + R_{\tau\theta pn}^k) - (D_{np})^T \left(R_{\tau,z \theta np}^k + R_{\tau,z \theta nn}^k\right)$$

$$+ \left(R_{\tau,z \theta np}^k + R_{\tau,z \theta nn}^k\right) \tag{17c}$$

$$\Pi_{u\theta}^{k\tau\theta} = (I_p)^T (R_{\tau\theta pp}^k + R_{\tau\theta pn}^k) + (I_{np})^T \left(R_{\tau,z \theta np}^k + R_{\tau,z \theta nn}^k\right) \tag{17d}$$

$$\tag{17e}$$
$$I_p = \begin{bmatrix} 1 & 0 & 0 \\ 0 & 1 & 0 \\ 1 & 1 & 0 \end{bmatrix}, \qquad I_{np} = \begin{bmatrix} 0 & 0 & 1 \\ 0 & 0 & 1 \\ 0 & 0 & 0 \end{bmatrix}$$

It can be verified that, in the case of simply supported plates, the natural boundary conditions are satisfied. Therefore, the governing equations can be written in the following compact form:

$$(\delta u_\tau^k)^T: \qquad K_{uu}^{k\tau s} u_s^k = K_{uT}^{k\tau\theta} T_\theta^k \tag{18}$$

$K_{uu}^{k\tau s}$ and $K_{uT}^{k\tau\theta}$ are 3×3 fundamental nuclei that can be automatically expanded trough the indexes θ, τ and s in order to obtained the governing differential equations of the desired refined plate model. The superscript k denotes the assembling on the number of layer.

ANALYTICAL SOLUTION

Navier type closed form solution are possible for simply supported plates, which satisfy the natural boundary conditions above. So, the displacement variables and the thermal load can be expressed in the following Fourier series.

$$u_{x_s}^k = \sum_{m,n} \left(U_{x_s}^k\right)\cos(\lambda x_k)\sin(\beta y_k), \qquad 0 \le x \le a; 0 \le y \le b$$

$$u_{y_s}^k = \sum_{m,n} \left(U_{y_s}^k\right)\sin(\lambda x_k)\cos(\beta y_k), \qquad 0 \le x \le a; 0 \le y \le b \qquad (19)$$

$$u_{z_s}^k = \sum_{m,n} \left(U_{z_s}^k\right)\sin(\lambda x_k)\sin(\beta y_k), \qquad 0 \le x \le a; 0 \le y \le b$$

$$T_\theta^k = \sum_{m,n} \left(\bar{T}_\theta^k\right)\sin(\lambda x_k)\sin(\beta y_k), \qquad 0 \le x \le a; 0 \le y \le b$$

where $\lambda = m\pi/a_k$ and $\beta = n\pi/b_k$. $U_{x_s}^k, U_{y_s}^k, U_{z_s}^k$ and $\bar{T}_\theta^k$ are amplitudes, m and n are the number of semi-waves. Therefore, the plate governing equations (Eq. 18) become

$$\begin{bmatrix} \bar{K}_{uu11}^{k\tau s} & \bar{K}_{uu12}^{k\tau s} & \bar{K}_{uu13}^{k\tau s} \\ \bar{K}_{uu21}^{k\tau s} & \bar{K}_{uu22}^{k\tau s} & \bar{K}_{uu23}^{k\tau s} \\ \bar{K}_{uu31}^{k\tau s} & \bar{K}_{uu32}^{k\tau s} & \bar{K}_{uu33}^{k\tau s} \end{bmatrix} \begin{bmatrix} U_{x_s}^k \\ U_{y_s}^k \\ U_{z_s}^k \end{bmatrix} = \begin{bmatrix} \bar{K}_{uT1}^{k\tau\theta} \\ \bar{K}_{uT2}^{k\tau\theta} \\ \bar{K}_{uT3}^{k\tau\theta} \end{bmatrix} \bar{T}_\theta^k \qquad (20)$$

where:

$$\bar{K}_{uu11}^{k\tau s} = \int_{A_k} \left(C_{55}^k(z)F_{\tau,z}F_{s,z} + \lambda^2 C_{11}^k(z)F_\tau F_s + \beta^2 C_{66}^k(z)F_\tau F_s\right)dz$$

$$\bar{K}_{uu12}^{k\tau s} = \int_{A_k} \left(\lambda\beta C_{12}^k(z)F_\tau F_s + \lambda\beta C_{66}^k(z)F_\tau F_s\right)dz$$

$$\bar{K}_{uu13}^{k\tau s} = \int_{A_k} \left(-\lambda C_{13}^k(z)F_\tau F_{s,z} + \lambda C_{55}^k(z)F_{\tau,z}F_s\right)dz$$

$$\overline{K}_{uu21}^{k\tau s} = \int_{A_k} \left(\lambda\beta C_{12}^k(z)F_\tau F_s + \lambda\beta C_{66}^k(z)F_\tau F_s \right)dz$$

$$\overline{K}_{uu22}^{k\tau s} = \int_{A_k} \left(C_{44}^k(z)F_{\tau_{,z}}F_{s_{,z}} + \beta^2 C_{22}^k(z)F_\tau F_s + \lambda^2 C_{66}^k(z)F_\tau F_s \right)dz$$

$$\overline{K}_{uu23}^{k\tau s} = \int_{A_k} \left(-\beta C_{23}^k(z)F_\tau F_{s_{,z}} + \beta C_{44}^k(z)F_{\tau_{,z}}F_s \right)dz$$

$$\overline{K}_{uu31}^{k\tau s} = \int_{A_k} \left(\lambda C_{55}^k(z)F_\tau F_{s_{,z}} - \lambda C_{13}^k(z)F_{\tau_{,z}}F_s \right)dz$$

$$\overline{K}_{uu32}^{k\tau s} = \int_{A_k} \left(\beta C_{44}^k(z)F_\tau F_{s_{,z}} - \beta C_{23}^k(z)F_{\tau_{,z}}F_s \right)dz$$

$$\overline{K}_{uu33}^{k\tau s} = \int_{A_k} \left(C_{33}^k(z)F_{\tau_{,z}}F_{s_{,z}} + \beta^2 C_{44}^k(z)F_\tau F_s + \lambda^2 C_{55}^k(z)F_\tau F_s \right)dz$$

$$\overline{K}_{uT1}^{k\tau\theta} = \int_{A_k} \left(\lambda\alpha F_\tau F_\theta \left(C_{11}^k(z) + C_{12}^k(z) + C_{13}^k(z) \right) \right)dz$$

$$\overline{K}_{uT2}^{k\tau\theta} = \int_{A_k} \left(\beta\alpha F_\tau F_\theta \left(C_{12}^k(z) + C_{22}^k(z) + C_{23}^k(z) \right) \right)dz$$

$$\overline{K}_{uT3}^{k\tau\theta} = \int_{A_k} \left(\alpha F_{\tau_{,z}}F_\theta \left(C_{13}^k(z) + C_{23}^k(z) + C_{33}^k(z) \right) \right)dz \qquad \text{(22a-l)}$$

The formal expressions of the fundamental stiffness nucleus, $\overline{K}_{uuij}^{k\tau s}$, and the fundamental thermomechanical stiffness nucleus, $\overline{K}_{uTi}^{k\tau\theta}$, do not depend on the theory kinematics and can be coded in a simple manner so as to obtain the final algebraic system of the desired model in an automatic manner.

NUMERICAL RESULTS

The thermoelastic bending analysis of simple supported FG sandwich plates is presented in what follows. Several plate theories within the CUF framework are developed. Different kinds of FG sandwich plates (see Fig. 2) are utilized in this work and they are described in Table 2. The structure is subjected to a bi-sinusoidal thermal load, $T_\theta^k = (\bar{T}_\theta)\sin(\lambda x)\sin(\beta y)$, with $\lambda = \pi/a$ and $\beta = \pi/b$. For this study, the following relations for non-dimensional deflections and stresses were adopted:

$$\bar{w} = \frac{h}{\alpha_0 \bar{T}_2 a^2} w\left(\frac{a}{2}, \frac{b}{2}, z\right), \qquad \bar{\sigma}_{xx} = \frac{h^2}{\alpha_0 \bar{T}_2 E_0 a^2} \sigma_{xx}\left(\frac{a}{2}, \frac{b}{2}, z\right)$$

$$\bar{\sigma}_{xz} = \frac{10h}{\alpha_0 \bar{T}_2 E_0 a} \sigma_{xz}\left(0, \frac{b}{2}, z\right), \qquad E_0 = 1 GPa, \qquad \alpha_0 = 10^{-6}{}^\circ C^{-1} \tag{23}$$

Numerical results of thermoelastic bending analysis of several plate models are presented in Tables 4 and 5using CUF. FG rectangular sandwich plates with various exponents "p" (see Eq. (1)), several side ratio "a/b" and different sandwich schemes are presented. Mechanical properties of the metal and ceramic used in the numerical examples are presented in Table 3. All results are obtained considering the ratio a/h=10. The results of the present work are compared with those from polynomial CUF models and the solution by Zenkour and Alghamdi [22]. A linear temperature distribution through the thickness ($T_1=T_3=0$, $T_2=100$) was utilized to obtain the results in Tables 4 and 5.

Tables 4 compares values of non-dimensional deflection $\bar{w}(z = 0)$ for different plate models (pol, $\sin^n$*(z/h)*, $\sin$*(nz/h)*, $\sec$*(z/h)*, *tanh(z/h)*, $\sinh^n$*(z/h)* and $\sinh$*(nz/h)*), various values of the exponent $p = \{0, 1, 2, 3, 4, 5\}$, $N = \{3, 7\}$ and different sandwich schemes. The normalized displacements fields ($\sin^n$*(z/h)*, $\sin$*(nz/h)*, $\sinh^n$*(z/h)*, $\sinh$*(nz/h)*

and tanh*(z/h)*) had a good agreement with the results from the literature and those from polynomial displacement fields (pol). Table 5 shows the results of non-dimensional deflection $\bar{w}(z=0)$ for different normalized displacements fields (pol, $\sin^n$*(z/h)*, sin*(nz/h)*, sec*(z/h)*, tanh*(z/h)*, $\sinh^n$*(z/h)* and sinh*(nz/h)*)), several values of the aspect ratio $a/b = \{1, 2, 3, 4, 5\}$, several sandwich schemes, N = {3,7} and $p = 3$.

Figures 3-15 show the non-dimensional axial stress $\bar{\sigma}_{xx}$ and shear stress $\bar{\sigma}_{xz}$ through the thickness for several displacement fields with different order of expansion (N={3,4,5,6,7}) of FG square sandwich plate (scheme (1-1-1), p=2 and a/h=10) for a linear temperature field ($\bar{T}_1=\bar{T}_3=0$, $\bar{T}_2=100$). The free surface bottom and top boundary conditions of the shear stress ($\bar{\sigma}_{xz}(z = -h/2, \; h/2) = 0$) are satisfied for N=7 in the polynomial and normalized non-polynomial displacement fields. However, non-normalized displacement fields ($\sin^n$*(z)*, sin*(nz)*, sec*(z)*, tanh*(z)*, $\sinh^n$*(z)* and sinh*(nz)*) don't satisfy this condition.

Results of the non-dimensional stress $\bar{\sigma}_{xx}$ and $\bar{\sigma}_{xz}$ for normalized non-polynomial models are compared with the results of the polynomial displacement field in Fig. 16 for a linear temperature field (p=2, a/h=10, $\bar{T}_1=\bar{T}_3=0$, $\bar{T}_2=100$, scheme (1-1-1)). The results are much close in the normalized case for N=7. Further, Fig 17 compares results from non-normalized displacement fields with those from the polynomial displacement field for N=7. Most of the theories with non-normalized shear strain functions ($\sin^n$*(z)*, sin*(nz)*, tanh*(z)*, $\sinh^n$*(z)* and sinh*(nz)*) have results which are close to each other. However, the results from the sec*(z)* model do not properly agree with the others. Further studies need to be carried out in order to know which approach performs best.

Fig. 18 presents the distribution of the dimensionless stresses $\bar{\sigma}_{xx}$ and $\bar{\sigma}_{xz}$ through the thickness direction of polynomial (pol) and sinusoidal (sin*(nz/h)*)

displacement field considering a nonlinear temperature distribution ($\psi_{(z)}$=(h/π)sin(πz/h), $\bar{T}_1$=0, $\bar{T}_2$=100) and different values of $\bar{T}_3$={-100,0,100}. This figure shows that values of stresses are very sensitive to the variation of the thermal load $\bar{T}_3$ and the form of the temperature distribution.

CONCLUSIONS

This paper presents an analytical solution for the thermoelastic bending analysis of simply supported functionally graded (FG) sandwich plates using Carrera's Unified Formulation with several shear strain functions of the non-polynomial form. Sinusoidal, hyperbolical and hybrid displacement fields are presented in this work in normalized and non-normalized form.

These new displacement fields had the capacity to reproduce the same results of the classical polynomial displacement field and further studies need to determinate which kinematics and polynomial or non-polynomial through-the-thickness expanding functions perform best within the context of the present formulation. However it is necessary take a special importance in the selection and normalization of the shear strain shape functions in any proposed displacement fields.

ACKNOWLEDGEMENT

REFERENCES

[1] M. Koizumi, The concept of FGM Ceramic transactions, Funct. Grad. Mater., vol. 34, pp. 3-10, 1993.

[2] H.T. Thai, S.E. Kim, A review of theories for the modeling and analysis of functionally graded plates and shells, Compos. Struct., vol. 128, pp. 70-86, 2015.

[3] K. Swaminathan, D.T. Naveenkumar, A.M. Zenkour, E. Carrera, Stress, vibration and buckling analysis of FGM plates – A state-of-art review, Compos. Struct. Vol 120, pp. 10-31, 2015.

[4] L. Demasi, ∞6 mixed plate theories based on the generalized unified formulation. Part I: Governing Equations, Compos. Struct., vol. 87, pp. 1-11, 2009.

[5] L. Demasi, ∞6 mixed plate theories based on the generalized unified formulation. Part II: Layerwise theories, Compos. Struct., vol. 87, pp. 12-22, 2009.

[6] L. Demasi, ∞6 mixed plate theories based on the generalized unified formulation. Part III: Advanced mixed high order shear deformation theories, Compos. Struct., vol. 87, pp. 183-194, 2009.

[7] L., Demasi, ∞6 mixed plate theories based on the generalized unified formulation. Part IV: Zig–zag theories, Compos. Struct., vol. 87, pp. 195-205, 2009.

[8] L. Demasi, ∞6 mixed plate theories based on the generalized unified formulation. Part V: Results, Compos. Struct., vol. 88, pp. 1-16, 2009.

[9] J.N. Reddy, C.F. Liu, A higher-order shear of deformation theory of laminated elastic shells, Int. J. Eng. Sci., vol. 23, pp. 319-330, 1985.

[10] J.N. Reddy, Analysis of functionally graded plates, Int. J. Numer. Meth. Eng., vol. 47, pp. 663-684, 2000.

[11] M. Touratier, An efficient standard plate theory, Int. J. Eng. Sci., vol. 29(8), pp. 901-916, 1991.

[12] K.P. Soldatos, A transverse shear deformation theory for homogeneous monoclinic plates, Acta Mech., vol. 94, pp. 195-220, 1992.

[13] A.M. Zenkour, Generalized shear deformation theory for bending analysis of functionally graded plates, Appl. Math. Model, vol. 30, pp. 67-84, 2006.

[14] A.M. Zenkour, Benchmark trigonometric and 3-D elasticity solutions for an exponentially graded thick rectangular plate, Appl. Math. Model, vol. 77, pp. 197-214, 2007.

[15] M. Karama, Mechanical behavior or laminated composite beam by the new multilayer laminated composite structures model with transverse shear stress continuity, Acta Mech., vol. 40, pp. 1525-1546, 2003.

[16] J.L. Mantari, A.S. Oktem, C. Guedes Soares, Bending response of functionally graded plates by using a new higher order shear deformation theory, Compos. Struct., vol. 94, pp. 714-723, 2012.

[17] J.L. Mantari, A.S. Oktem, C. Guedes Soares, Static and dynamic analysis of laminated composite and sandwich plates and shells by using a new higher order shear deformation theory, Compos. Struct., vol. 94, pp. 37-49, 2011.

[18] J.L. Mantari, A.S. Oktem, C. Guedes Soares, A new trigonometric deformation theory for isotropic, laminated composite and sandwich plates, Int. J. Solids Struct., vol. 49, pp. 43-53, 2012.

[19] J.L. Mantari, C. Guedes Soares, Bending analysis of thick exponentially graded plates using a new trigonometric higher order shear deformation theory, Compos. Struct., vol. 94, pp. 1991-2000, 2012.

[20] J.L. Mantari, E.V. Granados, C. Guedes Soares, Vibrational analysis of advanced composite plates resting on elastic foundation, Compos. B Eng., vol. 66, pp. 407-419, 2014.

[21] M.S.A. Houari, A. Tounsi, O. Anwar Bég, Thermoelastic bending analysis of functionally graded sandwich plates using a new higher order shear and normal deformation theory, Int. J. Mech. Sci., vol. 76 2013;76:102-11.

[22] A.M. Zenkour, N.A. Alghamdi, Thermoelastic bending analysis of functionally graded sandwich plates, J. Mater. Sci., vol. 43, pp. 2574-2589, 2008.

[23] J.L. Mantari, E.V. Grandos, Thermoelastic behavior of advanced composite sandwich plates by using a new quasi-3D hybrid type HSDT with 6 unknowns, Compos. Struc., vol. 126, pp. 132-144, 2015.

[24] E. Carrera, Evaluation of layer-wise mixed theories for laminated plate analysis, AIAA J., vol. 36, pp. 830-839, 1998.

[25] E. Carrera, Developments, ideas, and evaluations based upon Reissner's mixed variational theorem in the modelling of multilayered plates and shells, Appl. Mech. Rev., vol. 54, pp. 301-329, 2001.

[26] E. Carrera, Theories and finite elements for multilayered plates and shells: a unified compact formulation with numerical assessment and benchmarking, Arch. Comput. Methods Eng., vol. 10, pp. 215-296, 2003.

[27] M. Cinefra, S. Belouettar, M. Soave, E. Carrera, Variable kinematic models applied to free-vibration analysis of functionally graded material shells, Europ. J. Mech. A/Solids, vol. 29, pp. 1078-1087, 2010.

[28] A.J.M. Ferreira, E. Carrera, M. Cinefra, C.M.C. Roque, O. Polit, Analysis of laminated shells by a sinusoidal shear deformation theory and radial basis functions collocation, accounting for through-the-thickness deformations, Compos. B Eng., vol. 42(5), pp. 1276-1284, 2011.

[29] A.M.A. Neves, A.J.M. Ferreira, E. Carrera, C.M.C. Roque, M. Cinefra, R.M.N. Jorge, C.M.M. Soares, Bending of FGM plates by a sinusoidal plate formulation

and collocation with radial basis functions, Mech. Res. Commun., vol 38(5), pp. 368-371, 2011.

[30] A.M.A. Neves, A.J.M. Ferreira, E. Carrera, C.M.C. Roque, M. Cinefra, R.M.N. Jorge, C.M.M. Soares, A quasi-3D sinusoidal shear deformation theory for the static and free vibration analysis of functionally graded plates, Compos. B Eng., vol. 43(2), pp. 711-725, 2012.

[31] A.M.A. Neves, A.J.M. Ferreira, E. Carrera, M. Cinefra, C.M.C. Roque, R.M.N. Jorge, C.M.M. Soares, A quasi-3D hyperbolic shear deformation theory for the static and free vibration analysis of functionally graded plates, Compos. Struct., vol. 94(5), pp. 1814-1825, 2012.

[32] A.M.A. Neves, A.J.M. Ferreira, E. Carrera, M. Cinefra, C.M.C. Roque, R.M.N. Jorge, C.M.M. Soares, Buckling analysis of sandwich plates with functionally graded skins using anew quasi-3D hyperbolic sine shear deformation theory and collocation with radial basis function, ZAMM – J. Appl. Match. Mech./Z Angew. Match. Mech., 92(9), pp. 749-766, 2012.

[33] E. Carrera, M. Filippi, E. Zappino, Laminated beam analysis by polynomial, trigonometric, exponential and zig-zag theories, Eur. J. Mech. – A/Solids, vol. 41, pp. 58-69, 2013.

[34] M. Filippi, E. Carrera, A.M. Zenkour, Static analyses of FGM beams by various theories and finite elements, Compos. B Eng., vol. 72, pp. 1-9, 2015.

[35] D.S. Mashat, E. Carrera, A.M. Zenkour, S.A.A. Khateeb, M. Filippi, Free vibration of FGM layered beams by various theories and finite elements, Compos. B Eng., vol. 59(0), pp. 269-278, 2014.

[36] F.A. Fazzolari, E. Carrera,Thermal stability of FGM sandwich plates under various through-the-thickness temperature distributions. J. Therm. Stresses, vol 0, pp. 1-3, 2014.

[37] E. Carrera, S. Brishetto, M. Cinefra, M. Soave, Effects of thickness stretching in functionally graded plates and shells, Compos. B Eng., vol. 42(2), pp. 123-133, 2011.

Table Legends

Table 1. Through-the-thickness functions used for the kinematics of the 2D plate CUF models.

Table 2. Material proprieties for the case studies.

Table 3. Schemes of the FG sandwich plate.

Table 4. Dimensionless deflection $\bar{w}(z = 0)$ of FG sandwich plates (a/b=1, a/h=10, $\bar{T}_1=\bar{T}_3=0$, $\bar{T}_2=100$).

Table 5. Dimensionless deflection $\bar{w}(z = 0)$ of FG sandwich plates (p=3, a/h=10, $\bar{T}_1=\bar{T}_3=0$, $\bar{T}_2=100$).

Figure Captions

Figure 1. Geometry of functionally graded sandwich plate.

Figure 2. Functionally graded V_c along the thickness of a FG sandwich for different values of "p".

Figure 3. Dimensionless stresses $\bar{\sigma}_{xx}$ and $\bar{\sigma}_{xz}$ through the thickness direction of the polynomial (*pol*) displacement field and several N (p=2, a/h=10, $\bar{T}_1=\bar{T}_3=0$, $\bar{T}_2=100$, 1-1-1).

Figure 4. Dimensionless stresses $\bar{\sigma}_{xx}$ and $\bar{\sigma}_{xz}$ through the thickness direction of the normalized sinusoidal ($\sin^n(z/h)$) displacement field and several N (p=2, a/h=10, $\bar{T}_1=\bar{T}_3=0$, $\bar{T}_2=100$, 1-1-1).

Figure 5. Dimensionless stresses $\bar{\sigma}_{xx}$ and $\bar{\sigma}_{xz}$ through the thickness direction of the non-normalized sinusoidal ($\sin^n(z)$) displacement field and several N (p=2, a/h=10, $\bar{T}_1=\bar{T}_3=0$, $\bar{T}_2=100$, 1-1-1).

Figure 6. Dimensionless stresses $\bar{\sigma}_{xx}$ and $\bar{\sigma}_{xz}$ through the thickness direction of the normalized sinusoidal ($\sin(nz/h)$) displacement field and several N (p=2, a/h=10, $\bar{T}_1=\bar{T}_3=0$, $\bar{T}_2=100$, 1-1-1).

Figure 7. Dimensionless stresses $\bar{\sigma}_{xx}$ and $\bar{\sigma}_{xz}$ through the thickness direction of the non-normalized sinusoidal ($\sin(nz)$) displacement field and several N (p=2, a/h=10, $\bar{T}_1=\bar{T}_3=0$, $\bar{T}_2=100$, 1-1-1).

Figure 8. Dimensionless stresses $\bar{\sigma}_{xx}$ and $\bar{\sigma}_{xz}$ through the thickness direction of the normalized hybrid ($\sec(z/h)$) displacement field and several N (p=2, a/h=10, $\bar{T}_1=\bar{T}_3=0$, $\bar{T}_2=100$, 1-1-1).

Figure 9. Dimensionless stresses $\bar{\sigma}_{xx}$ and $\bar{\sigma}_{xz}$ through the thickness direction of the non-normalized hybrid ($\sec(z)$) displacement field and several N (p=2, a/h=10, $\bar{T}_1=\bar{T}_3=0$, $\bar{T}_2=100$, 1-1-1).

Figure 10. Dimensionless stresses $\bar{\sigma}_{xx}$ and $\bar{\sigma}_{xz}$ through the thickness direction of the normalized hybrid ($\tanh(z/h)$) displacement field and several N (p=2, a/h=10, $\bar{T}_1=\bar{T}_3=0$, $\bar{T}_2=100$, 1-1-1).

Figure 11. Dimensionless stresses $\bar{\sigma}_{xx}$ and $\bar{\sigma}_{xz}$ through the thickness direction of the non-normalized hybrid ($\tanh(z)$) displacement field and several N (p=2, a/h=10, $\bar{T}_1=\bar{T}_3=0$, $\bar{T}_2=100$, 1-1-1).

Figure 12. Dimensionless stresses $\bar{\sigma}_{xx}$ and $\bar{\sigma}_{xz}$ through the thickness direction of the normalized hyperbolical (sinh^n(z/h)) displacement field and several N (p=2, a/h=10, $\bar{T}_1=\bar{T}_3=0$, $\bar{T}_2=100$, 1-1-1).

Figure 13. Dimensionless stresses $\bar{\sigma}_{xx}$ and $\bar{\sigma}_{xz}$ through the thickness direction of the non-normalized hyperbolical (sinh^n(z)) displacement field and several N (p=2, a/h=10, $\bar{T}_1=\bar{T}_3=0$, $\bar{T}_2=100$, 1-1-1).

Figure 14. Dimensionless stresses $\bar{\sigma}_{xx}$ and $\bar{\sigma}_{xz}$ through the thickness direction of the normalized hyperbolical (sinh(nz/h)) displacement field and several N (p=2, a/h=10, $\bar{T}_1=\bar{T}_3=0$, $\bar{T}_2=100$, 1-1-1).

Figure 15. Dimensionless stresses $\bar{\sigma}_{xx}$ and $\bar{\sigma}_{xz}$ through the thickness direction of the non-normalized hyperbolical (sinh(nz)) displacement field and several N (p=2, a/h=10, $\bar{T}_1=\bar{T}_3=0$, $\bar{T}_2=100$, 1-1-1).

Figure 16. Dimensionless stresses $\bar{\sigma}_{xx}$ and $\bar{\sigma}_{xz}$ through the thickness direction of several normalized displacement fields (p=2, N=7, a/h=10, $\bar{T}_1=\bar{T}_3=0$, $\bar{T}_2=100$, 1-1-1).

Figure 17. Dimensionless stresses $\bar{\sigma}_{xx}$ and $\bar{\sigma}_{xz}$ through the thickness direction of several non-normalized displacement fields (p=2, N=7, a/h=10, $\bar{T}_1=\bar{T}_3=0$, $\bar{T}_2=100$, 1-1-1).

Figure 18. Dimensionless stresses $\bar{\sigma}_{xx}$ and $\bar{\sigma}_{xz}$ through the thickness direction of polynomial (pol) and sinusoidal (sin(nz/h)) displacement field considering a nonlinear temperature distribution ($\psi_{(z)}$=(h/π)sin(πz/h), p=2, N=7, a/h=10, $\bar{T}_1=0$, $\bar{T}_2=100$, 1-1-1).

Tables

Table 1.

	$f_{0(z)}$	$f_{1(z)}$	$f_{2(z)}$	$f_{3(z)}$	$f_{4(z)}$	$f_{5(z)}$	$f_{6(z)}$	$f_{7(z)}$
Pol	1	z	z^2	z^3	z^4	z^5	z^6	z^7
$\sin^n(z/h)$	1	z	$\cos(z/h)$	$\sin(z/h)$	$\cos^2(z/h)$	$\sin^3(z/h)$	$\cos^3(z/h)$	$\sin^5(z/h)$
$\sin^n(z)$	1	z	$\cos(z)$	$\sin(z)$	$\cos^2(z)$	$\sin^3(z)$	$\cos^3(z)$	$\sin^5(z)$
$\sin(nz/h)$	1	z	$\cos(z/h)$	$\sin(z/h)$	$\cos(2z/h)$	$\sin(2z/h)$	$\cos(3z/h)$	$\sin(3z/h)$
$\sin(nz)$	1	z	$\cos(z)$	$\sin(z)$	$\cos(2z)$	$\sin(2z)$	$\cos(3z)$	$\sin(3z)$
$\sec(z/h)$	1	z	$\sec(z/h)$	$ze^{(z/h)^2}$	$\sec^2(z/h)$	$z^3 e^{(z/h)^2}$	$\sec^3(z/h)$	$z^5 e^{(z/h)^2}$
$\sec(z)$	1	z	$\sec(z)$	ze^{z^2}	$\sec^2(z)$	$z^3 e^{z^2}$	$\sec^3(z)$	$z^5 e^{z^2}$
$\tanh(z/h)$	1	z	$\cos(z/h)$	$\tanh(z/h)$	$\cos(2z/h)$	$\tanh(2z/h)$	$\cos(3z/h)$	$\tanh(3z/h)$
$\tanh(z)$	1	z	$\cos(z)$	$\tanh(z)$	$\cos(2z)$	$\tanh(2z)$	$\cos(3z)$	$\tanh(3z)$
$\sinh^n(z/h)$	1	z	$\cosh(z/h)$	$\sinh(z/h)$	$\cosh^2(z/h)$	$\sinh^3(z/h)$	$\cosh^3(z/h)$	$\sinh^5(z/h)$
$\sinh^n(z)$	1	z	$\cosh(z)$	$\sinh(z)$	$\cosh^2(z)$	$\sin^3(z)$	$\cos^3(z)$	$\sin^5(z)$
$\sinh(nz/h)$	1	z	$\cosh(z/h)$	$\sinh(z/h)$	$\cosh(2z/h)$	$\sinh(2z/h)$	$\cosh(3z/h)$	$\sinh(3z/h)$
$\sinh(nz)$	1	z	$\cosh(z)$	$\sinh(z)$	$\cosh(2z)$	$\sinh(2z)$	$\cosh(3z)$	$\sinh(3z)$

Table 2.

Scheme	h_2	h_3
1-0-1	0	0
1-1-1	$-h/6$	$h/6$
1-2-1	$-h/4$	$h/4$
2-1-2	$-h/10$	$h/10$
2-2-1	$-h/10$	$3h/10$

Table 3.

Material	Properties		
	E(GPa)	ν	$\alpha\ (10^{-6}/K)$
Metal (Ti-6Al-4V)	70	1/3	10.3
Ceramic (ZrO$_2$)	380	1/3	7.11

Table 4.

p	Theory	$\overline{w}$									
		1-0-1		1-1-1		1-2-1		2-1-2		2-2-1	
		N=3	N=7	N=3	N=7	N=3	N=7	N=3	N=7	N=3	N=7
0	Zenkour et al.[22]	0.461634	-	0.461634	-	0.461634	-	0.461634	-	0.461634	-
	Present – pol	0.448019	0.448017	0.448019	0.448017	0.448019	0.448017	0.448019	0.448017	0.448019	0.448017
	Present - $\sin^n(z/h)$	0.448011	0.448017	0.448011	0.448017	0.448011	0.448017	0.448011	0.448017	0.448011	0.448017
	Present -$\sin(nz/h)$	0.448011	0.448017	0.448011	0.448017	0.448011	0.448017	0.448011	0.448017	0.448011	0.448017
	Present -$\sec(z/h)$	0.448716	0.450233	0.448716	0.450233	0.448716	0.450233	0.448716	0.450233	0.448716	0.450233
	Present -$\tanh(z/h)$	0.448009	0.448017	0.448009	0.448017	0.448009	0.448017	0.448009	0.448017	0.448009	0.448017
	Present -$\sinh^n(z/h)$	0.448066	0.448017	0.448066	0.448017	0.448066	0.448017	0.448066	0.448017	0.448066	0.448017
	Present -$\sinh(nz/h)$	0.448066	0.448017	0.448066	0.448017	0.448066	0.448017	0.448066	0.448017	0.448066	0.448017
1	Zenkour et al.[22]	0.614565	-	0.586124	-	0.563416	-	0.599933	-	0.573327	-
	Present –pol	0.594285	0.594574	0.565759	0.566153	0.543453	0.54384	0.579548	0.579901	0.552994	0.553330
	Present -$\sin^n(z/h)$	0.594508	0.594575	0.566088	0.566154	0.543822	0.543839	0.579830	0.579902	0.553324	0.553329
	Present -$\sin(nz/h)$	0.594508	0.594575	0.566088	0.566154	0.543822	0.543839	0.579830	0.579902	0.553324	0.553329
	Present -$\sec(z/h)$	0.594056	0.516102	0.564939	0.453433	0.542353	0.414865	0.578994	0.482361	0.552118	0.437938
	Present -$\tanh(z/h)$	0.594502	0.594575	0.566090	0.566154	0.543831	0.543839	0.579827	0.579902	0.553327	0.553330
	Present -$\sinh^n(z/h)$	0.594122	0.594573	0.565490	0.566152	0.543141	0.543841	0.579326	0.579900	0.552722	0.553331
	Present -$\sinh(nz/h)$	0.594122	0.594573	0.565490	0.566152	0.543141	0.543841	0.579326	0.579900	0.552722	0.553331
2	Zenkour et al.[22]	0.647135	-	0.618046	-	0.590491	-	0.633340	-	0.601843	-
	Present –pol	0.626506	0.626743	0.596582	0.597037	0.569143	0.569652	0.612203	0.612559	0.580018	0.580411
	Present -$\sin^n(z/h)$	0.626650	0.626746	0.596908	0.59704	0.569564	0.569652	0.612442	0.612563	0.580367	0.580411
	Present -$\sin(nz/h)$	0.626650	0.626746	0.596908	0.597039	0.569564	0.569652	0.612442	0.612563	0.580367	0.58041
	Present -$\sec(z/h)$	0.626767	0.576272	0.595892	0.491307	0.567877	0.432319	0.611981	0.532927	0.579129	0.463732
	Present -$\tanh(z/h)$	0.626636	0.626746	0.596905	0.597039	0.569573	0.569651	0.612431	0.612563	0.580368	0.580412
	Present -$\sinh^n(z/h)$	0.626425	0.626743	0.596322	0.597035	0.568786	0.569653	0.612029	0.612558	0.579731	0.58041
	Present -$\sinh(nz/h)$	0.626425	0.626743	0.596322	0.597035	0.568786	0.569652	0.612029	0.612558	0.579731	0.58041
3	Zenkour et al.[22]	0.658153	-	0.631600	-	0.602744	-	0.646475	-	0.614121	-
	Present –pol	0.637735	0.637903	0.609903	0.610348	0.580873	0.581425	0.625356	0.625667	0.591749	0.59214
	Present -$\sin^n(z/h)$	0.637819	0.637906	0.610199	0.610352	0.581299	0.581426	0.625543	0.625671	0.592087	0.59214
	Present -$\sin(nz/h)$	0.637819	0.637907	0.610199	0.610351	0.581299	0.579635	0.625543	0.625671	0.592087	0.59214
	Present -$\sec(z/h)$	0.638312	0.607241	0.609422	0.51597	0.581306	0.581423	0.625436	0.562998	0.590964	0.48097
	Present -$\tanh(z/h)$	0.637801	0.637905	0.610191	0.610352	0.580513	0.581425	0.625526	0.625671	0.592085	0.592143
	Present -$\sinh^n(z/h)$	0.637713	0.637903	0.609676	0.610345	0.580513	0.581425	0.625235	0.625665	0.591475	0.592139
	Present -$\sinh(nz/h)$	0.637713	0.637903	0.609676	0.610345	0.580513	0.581424	0.625235	0.625665	0.591475	0.592139
4	Zenkour et al.[22]	0.662811	-	0.638705	-	0.609560	-	0.652890	-	0.620663	-
	Present –pol	0.642597	0.642715	0.616991	0.617413	0.587449	0.588017	0.631911	0.632178	0.598048	0.598426
	Present -$\sin^n(z/h)$	0.642646	0.642719	0.617259	0.617418	0.587871	0.588018	0.632061	0.632183	0.598373	0.598426
	Present -$\sin(nz/h)$	0.642646	0.642719	0.617259	0.617417	0.587871	0.588019	0.632061	0.632183	0.598373	0.598426
	Present -$\sec(z/h)$	0.643349	0.623854	0.616675	0.531873	0.586268	0.456759	0.632193	0.581370	0.597355	0.492106
	Present -$\tanh(z/h)$	0.642626	0.642717	0.617248	0.617419	0.587877	0.588015	0.63204	0.632182	0.598368	0.598429
	Present -$\sinh^n(z/h)$	0.642609	0.642715	0.616792	0.617409	0.587095	0.588016	0.631828	0.632176	0.597789	0.598424
	Present -$\sinh(nz/h)$	0.642609	0.642715	0.616792	0.61741	0.587095	0.588016	0.631828	0.632176	0.597789	0.598424
5	Zenkour et al.[22]	0.665096	-	0.642948	-	0.613842	-	0.656490	-	0.624629	-
	Present –pol	0.645027	0.645113	0.621275	0.621674	0.591606	0.59218	0.635651	0.635884	0.601893	0.602256
	Present -$\sin^n(z/h)$	0.645056	0.645115	0.621522	0.621679	0.592022	0.592182	0.635774	0.635889	0.602206	0.602257
	Present -$\sin(nz/h)$	0.645056	0.645116	0.621522	0.621679	0.592022	0.592182	0.635774	0.635889	0.602206	0.602257
	Present -$\sec(z/h)$	0.645878	0.633357	0.621079	0.542665	0.590478	0.463931	0.636068	0.593300	0.601270	0.499655
	Present -$\tanh(z/h)$	0.645036	0.645114	0.621507	0.621682	0.592026	0.592177	0.63575	0.635888	0.602200	0.60226
	Present -$\sinh^n(z/h)$	0.645059	0.645113	0.621097	0.62167	0.591259	0.592178	0.635593	0.635882	0.601645	0.602255
	Present -$\sinh(nz/h)$	0.645059	0.645113	0.621097	0.621671	0.591259	0.592178	0.635593	0.635882	0.601645	0.602255

Table 5.

| Scheme	Theory	$\bar{w}$									
		a/b=1		a/b=2		a/b=3		a/b=4		a/b=5	
		N=3	N=7	N=3	N=7	N=3	N=7	N=3	N=7	N=3	N=7
1-0-1	Zenkour et al.[22]	0.658153	-	0.270902	-	0.141810	-	0.088642	-	0.062334	-
	Present –pol	0.637735	0.637903	0.253276	0.253442	0.125113	0.125276	0.072328	0.072486	0.046213	0.046367
	Present -$\sin^n$(z/h)	0.637819	0.637906	0.253285	0.253446	0.125097	0.125279	0.072301	0.072490	0.046181	0.046370
	Present -sin(nz/h)	0.637819	0.637907	0.253285	0.253446	0.125097	0.125279	0.072301	0.072490	0.046181	0.046370
	Present -sec(z/h)	0.638312	0.607241	0.253643	0.242886	0.125411	0.121451	0.072600	0.071449	0.046473	0.046723
	Present -tanh(z/h)	0.637905	0.253267	0.253267	0.253445	0.125078	0.125278	0.072282	0.072489	0.046161	0.046369
	Present -$\sinh^n$(z/h)	0.637713	0.637903	0.253292	0.253442	0.125276	0.072362	0.072486	0.072486	0.046250	0.046367
	Present -sinh(nz/h)	0.637713	0.637903	0.253292	0.253442	0.125142	0.125275	0.072362	0.072486	0.046250	0.046367
1-1-1	Zenkour et al.[22]	0.631600	-	0.259980	-	0.136105	-	0.085094	-	0.059862	-
	Present –pol	0.609903	0.610348	0.242372	0.242814	0.119851	0.120289	0.069388	0.069821	0.044420	0.044848
	Present -$\sin^n$(z/h)	0.610199	0.610352	0.242470	0.242818	0.119883	0.120292	0.069393	0.069825	0.044411	0.044851
	Present -sin(nz/h)	0.610199	0.610351	0.242470	0.242818	0.119883	0.120292	0.069393	0.069824	0.044411	0.044851
	Present -sec(z/h)	0.609422	0.515970	0.242288	0.206401	0.119901	0.103238	0.069496	0.060763	0.044559	0.039759
	Present -tanh(z/h)	0.610191	0.610352	0.242462	0.242819	0.119874	0.120293	0.069383	0.069825	0.044401	0.044852
	Present -$\sinh^n$(z/h)	0.609676	0.610345	0.242301	0.242811	0.119832	0.120286	0.069391	0.069818	0.044435	0.044844
	Present -sinh(nz/h)	0.609676	0.610345	0.242301	0.242811	0.119832	0.120286	0.069391	0.069818	0.044435	0.044845
1-2-1	Zenkour et al.[22]	0.602744	-	0.248135	-	0.129933	-	0.081262	-	0.057192	-
	Present –pol	0.580873	0.581425	0.230967	0.231517	0.114318	0.114863	0.066270	0.066809	0.042493	0.043024
	Present -$\sin^n$(z/h)	0.581299	0.581426	0.231122	0.231517	0.114382	0.114863	0.066297	0.066809	0.042500	0.043025
	Present -sin(nz/h)	0.581299	0.581426	0.231122	0.231517	0.114382	0.114863	0.066297	0.066809	0.042500	0.043025
	Present -sec(z/h)	0.579635	0.446684	0.230552	0.178739	0.114180	0.089417	0.066248	0.052636	0.042531	0.034447
	Present -tanh(z/h)	0.581306	0.581423	0.231129	0.231515	0.114389	0.114861	0.066302	0.066806	0.042504	0.043022
	Present -$\sinh^n$(z/h)	0.580513	0.581425	0.230839	0.231516	0.114267	0.114862	0.066251	0.066808	0.042490	0.043024
	Present -sinh(nz/h)	0.580513	0.581424	0.230839	0.231516	0.114267	0.114862	0.066251	0.066808	0.042490	0.043023
2-1-2	Zenkour et al.[22]	0.646475	-	0.266094	-	0.139295	-	0.087077	-	0.061244	-
	Present –pol	0.625356	0.625667	0.248430	0.248739	0.122779	0.123084	0.071029	0.071329	0.045426	0.045722
	Present -$\sin^n$(z/h)	0.625543	0.625671	0.248482	0.248743	0.122786	0.123088	0.071016	0.071333	0.045404	0.045726
	Present -sin(nz/h)	0.625543	0.625671	0.248482	0.248743	0.122786	0.123088	0.071016	0.071333	0.045404	0.045726
	Present -sec(z/h)	0.625436	0.562998	0.248589	0.225193	0.122965	0.112619	0.071228	0.066269	0.045634	0.043349
	Present -tanh(z/h)	0.625526	0.625671	0.248465	0.248743	0.122768	0.123088	0.070998	0.071333	0.045386	0.045726
	Present -$\sinh^n$(z/h)	0.625235	0.625665	0.248404	0.248736	0.122785	0.123081	0.071048	0.071327	0.045453	0.045720
	Present -sinh(nz/h)	0.625235	0.625665	0.248404	0.248736	0.122785	0.123081	0.071048	0.071327	0.045453	0.045720
2-2-1	Zenkour et al.[22]	0.614121	-	0.252758	-	0.132303	-	0.082701	-	0.058168	-
	Present –pol	0.591749	0.592140	0.235212	0.235601	0.116355	0.116740	0.067400	0.067781	0.043177	0.043552
	Present -$\sin^n$(z/h)	0.592087	0.592140	0.235329	0.235602	0.116398	0.116741	0.067413	0.067781	0.043174	0.043553
	Present -sin(nz/h)	0.592087	0.592140	0.235329	0.235601	0.116398	0.116741	0.067413	0.067781	0.043174	0.043553
	Present -sec(z/h)	0.590964	0.480970	0.234996	0.192473	0.116330	0.096307	0.067456	0.056718	0.043275	0.037152
	Present -tanh(z/h)	0.592085	0.592143	0.235327	0.235604	0.116395	0.116743	0.067408	0.067784	0.043169	0.043556
	Present -$\sinh^n$(z/h)	0.591475	0.592139	0.235121	0.235600	0.116325	0.116739	0.067396	0.067780	0.043185	0.043552
	Present -sinh(nz/h)	0.591475	0.592139	0.592139	0.235600	0.116325	0.116739	0.067396	0.067780	0.043185	0.043552

Figures

Figure 1.
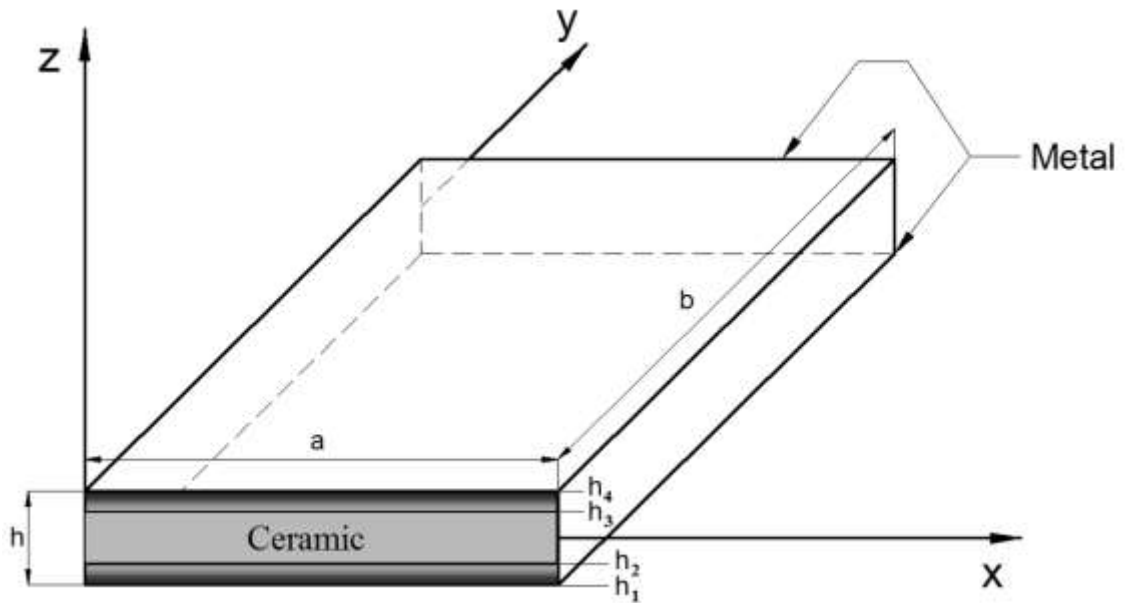
Figure 2.
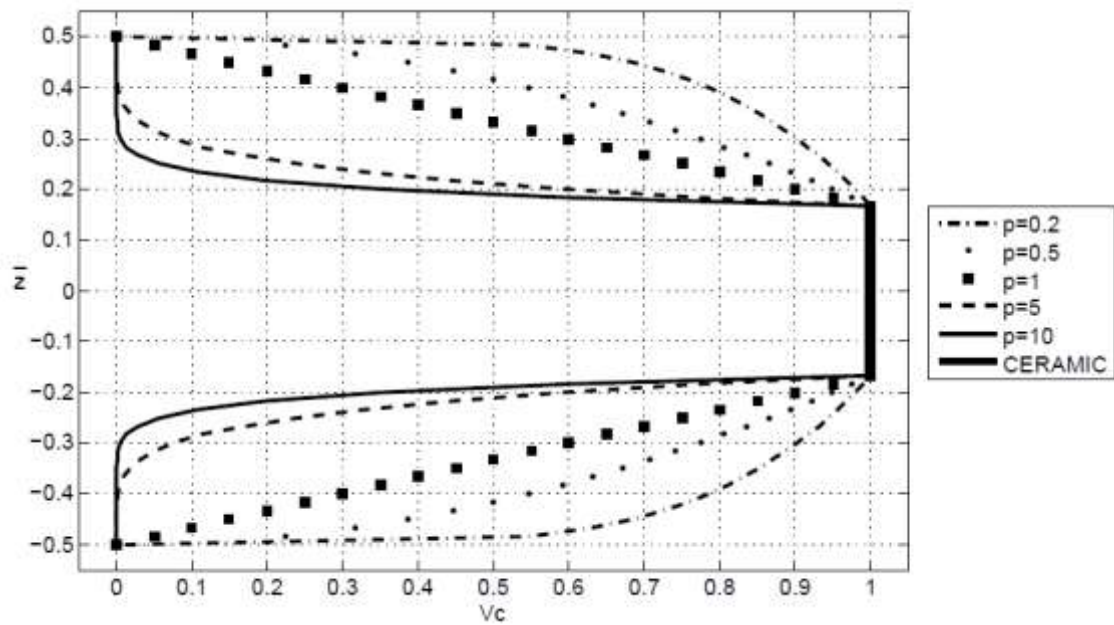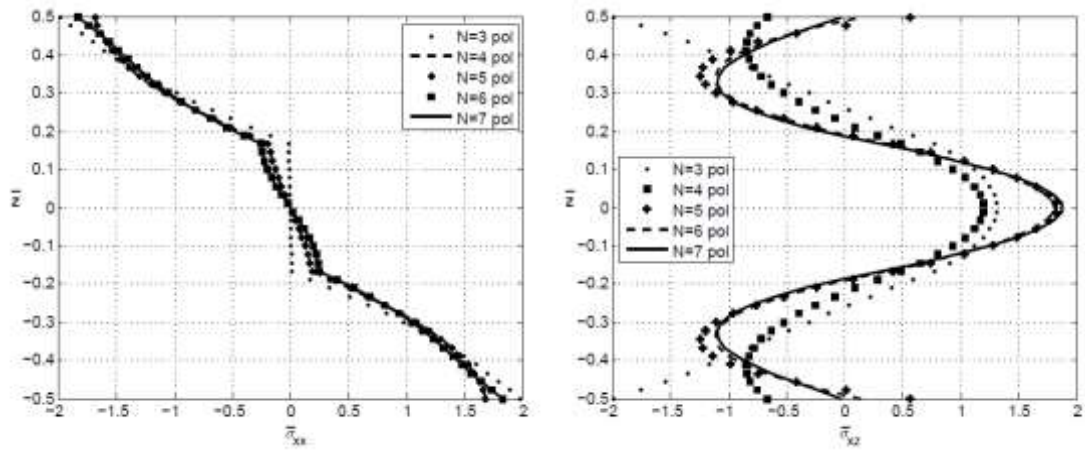
Figure 3.

Figure 4.
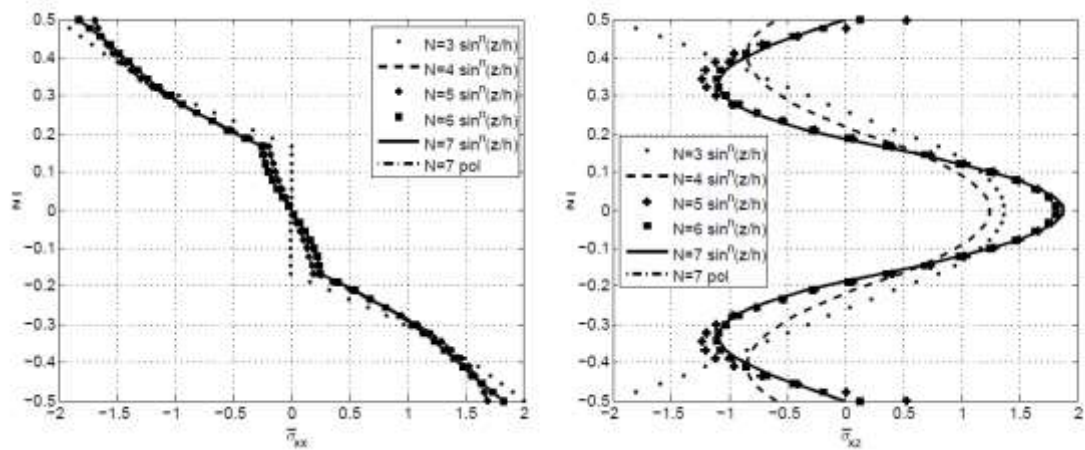
Figure 5.
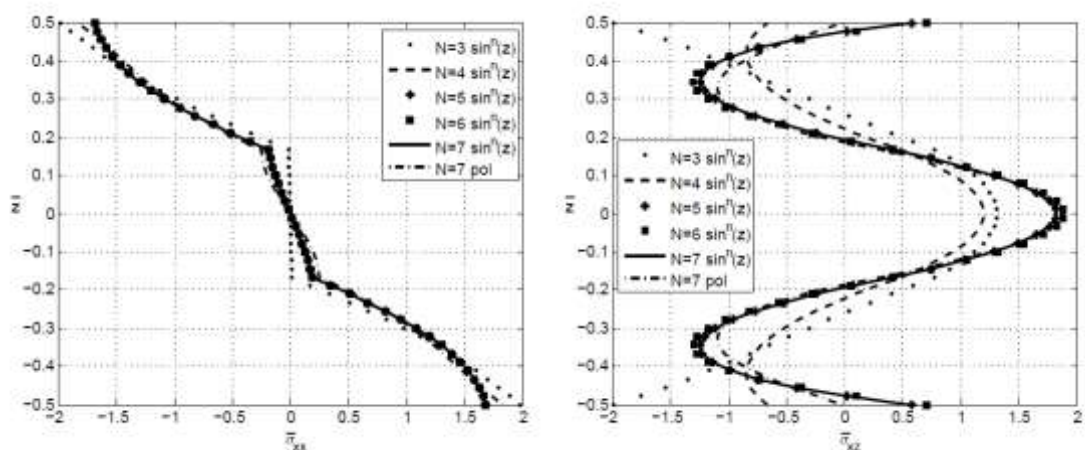
Figure 6.
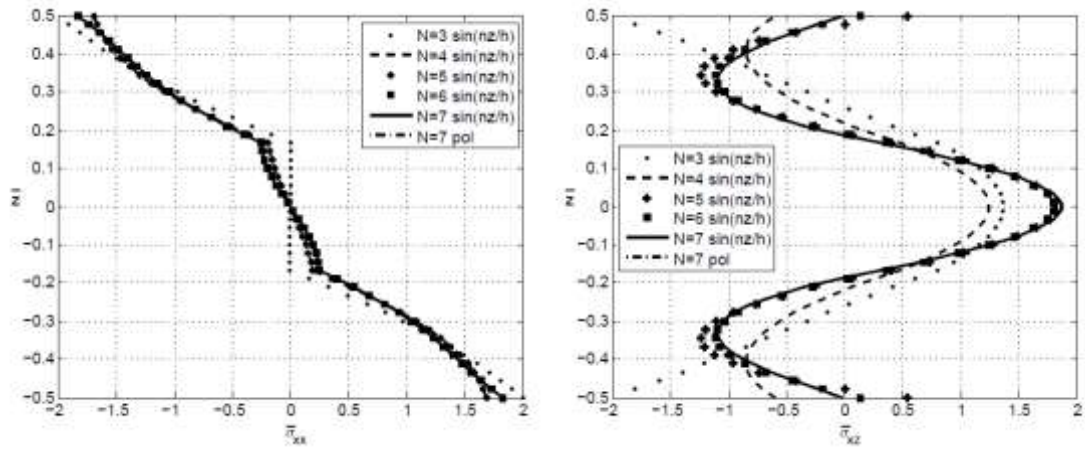
Figure 7.
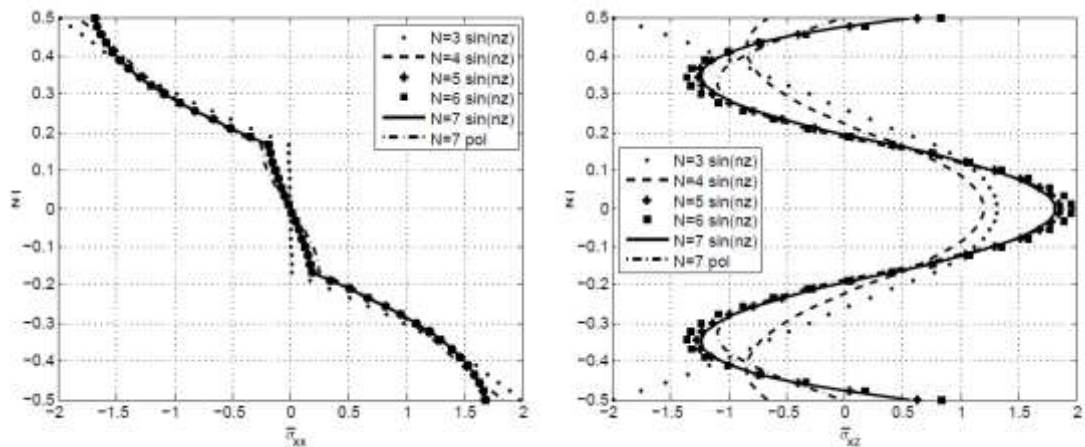
Figure 8.
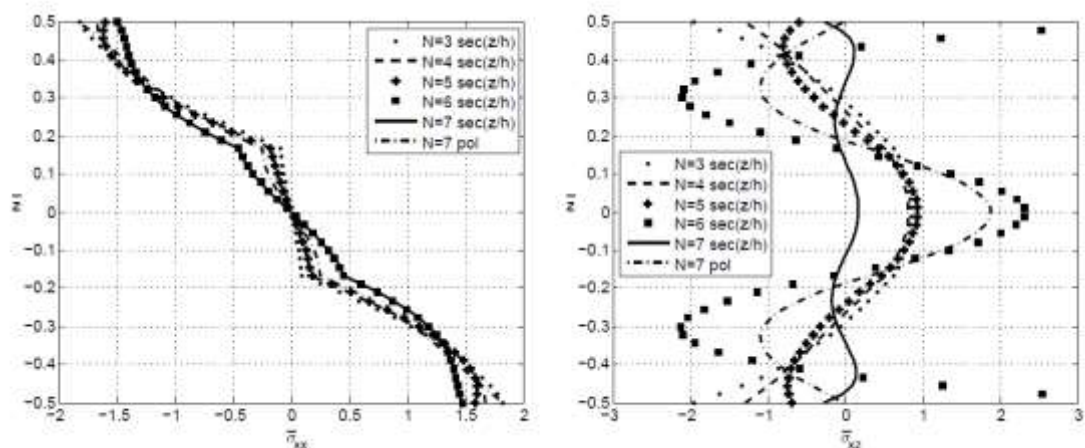
Figure 9.
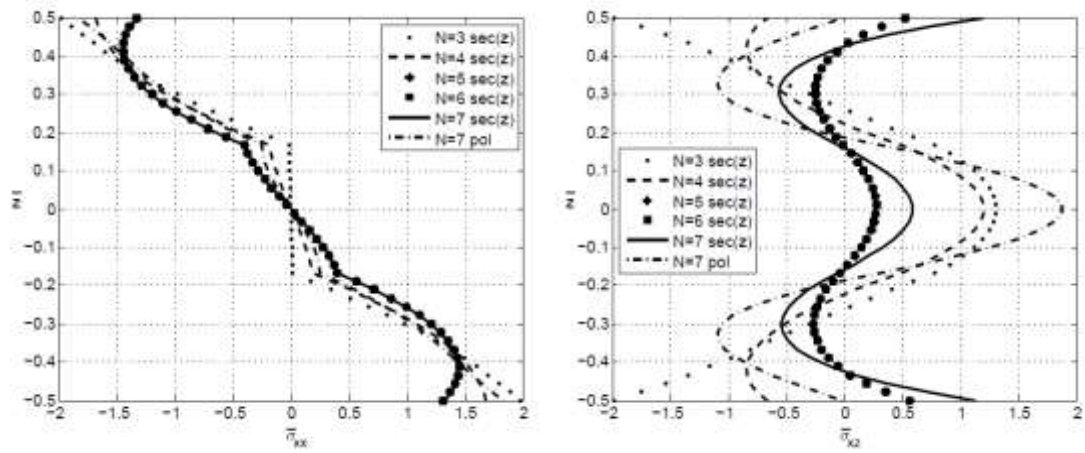
Figure 10.
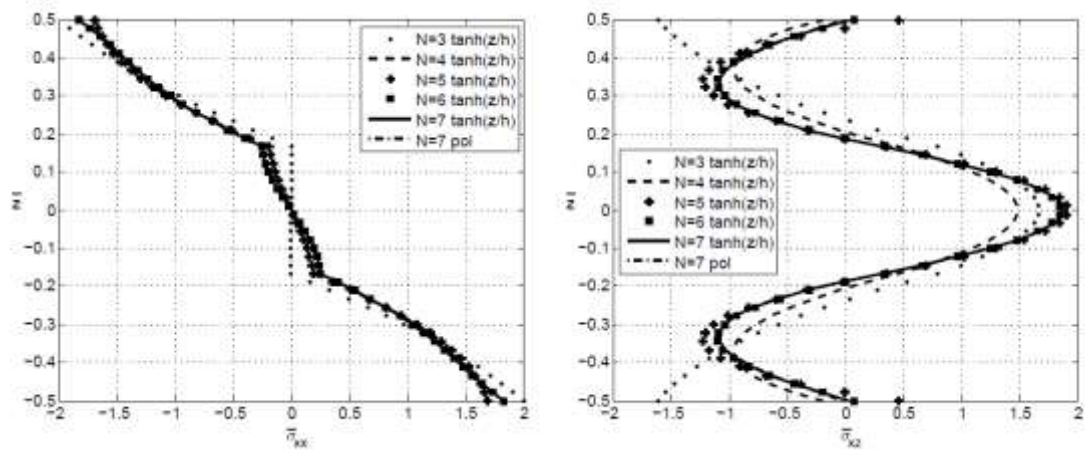
Figure 11.
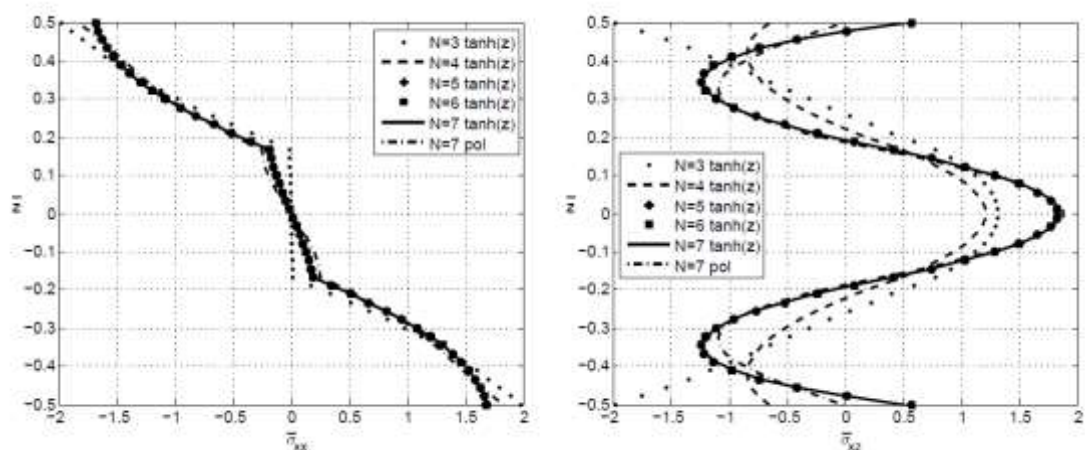
Figure 12.
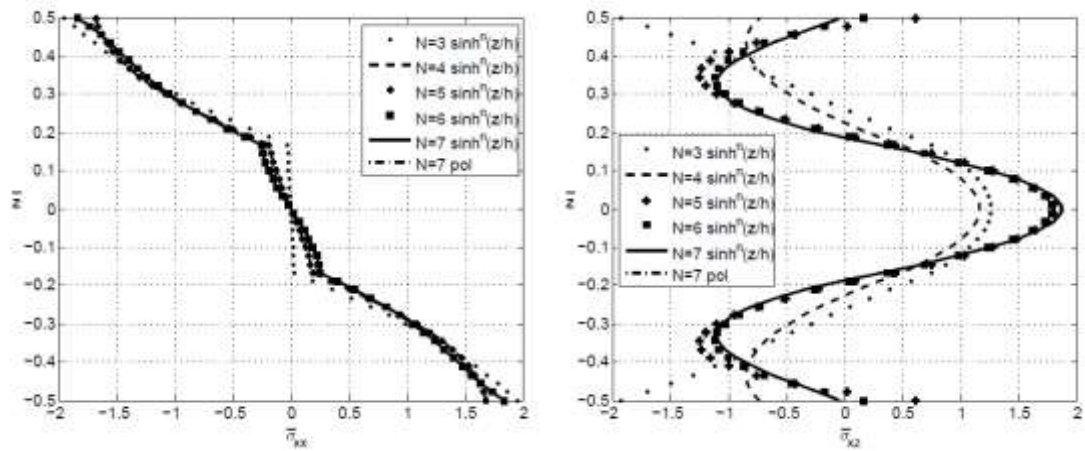
Figure 13.
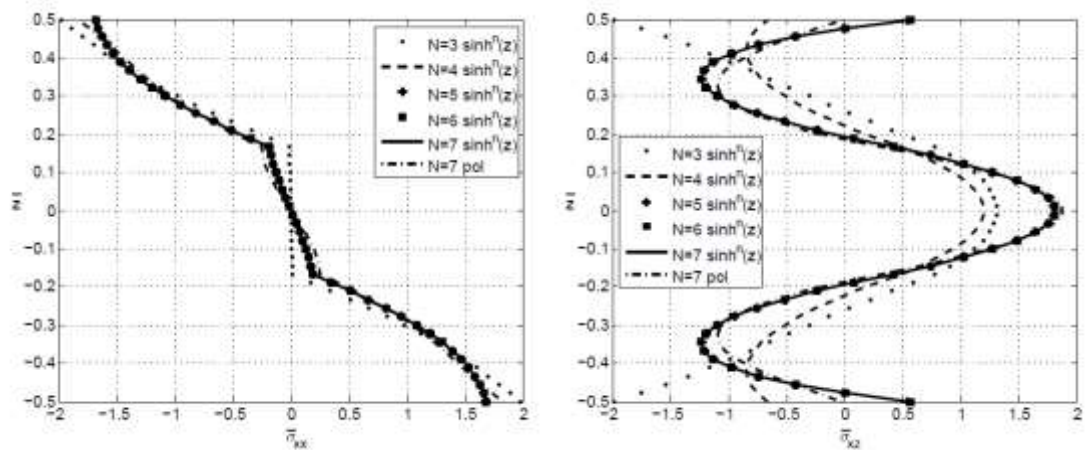
Figure 14.
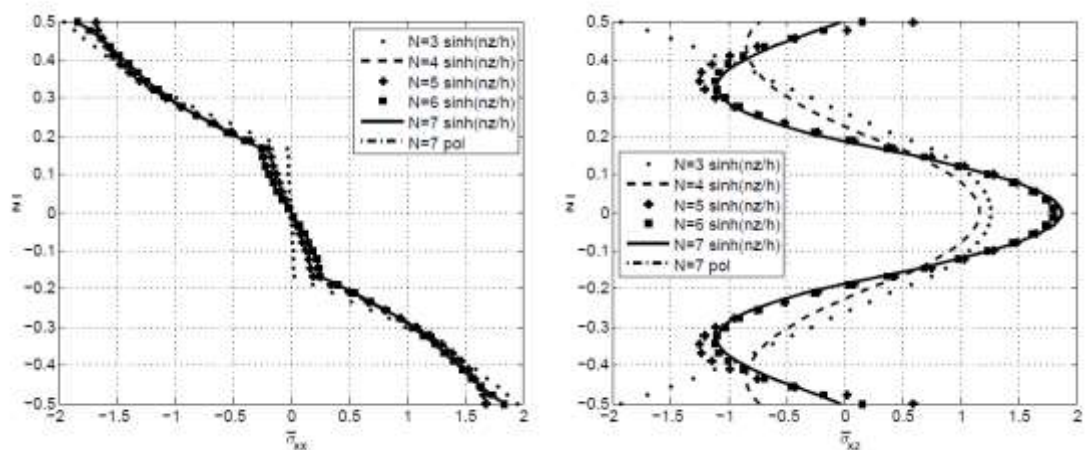
Figure 15.
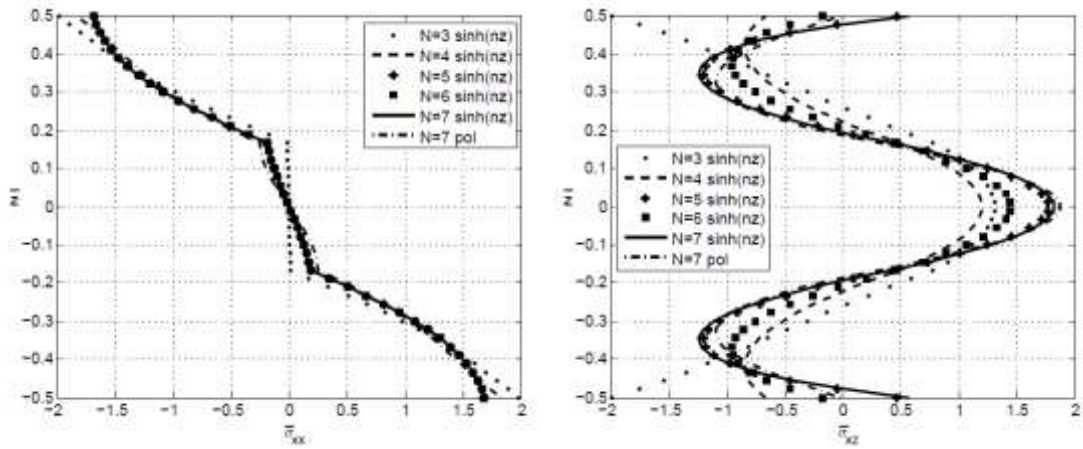
Figure 16.

Figure 17.

Figure 18.